



Deposited via The University of York.

White Rose Research Online URL for this paper:

<https://eprints.whiterose.ac.uk/id/eprint/130472/>

Version: Accepted Version

Article:

Leake, Mark Christian (2018) Transcription factors in eukaryotic cells can functionally regulate gene expression by acting in oligomeric assemblies formed from an intrinsically disordered protein phase transition enabled by molecular crowding. *Transcription*. pp. 298-306.

<https://doi.org/10.1080/21541264.2018.1475806>

Reuse

This article is distributed under the terms of the Creative Commons Attribution (CC BY) licence. This licence allows you to distribute, remix, tweak, and build upon the work, even commercially, as long as you credit the authors for the original work. More information and the full terms of the licence here:

<https://creativecommons.org/licenses/>

Takedown

If you consider content in White Rose Research Online to be in breach of UK law, please notify us by emailing eprints@whiterose.ac.uk including the URL of the record and the reason for the withdrawal request.

Transcription

Transcription factors in eukaryotic cells can functionally regulate gene expression by acting in oligomeric assemblies formed from an intrinsically disordered protein phase transition enabled by molecular crowding

--Manuscript Draft--

Manuscript Number:	KTRN-2018-0012R1
Article Type:	Point-of-View
Keywords:	gene expression; transcription factors; single-molecule; super-resolution; cell signaling; intrinsically disordered protein; phase transition; molecular crowding; fluorescent protein
Corresponding Author:	Mark Leake UNITED KINGDOM
First Author:	Mark Leake
Order of Authors:	Mark Leake
Manuscript Region of Origin:	UNITED KINGDOM
Abstract:	High-speed single-molecule fluorescence microscopy in vivo shows that transcription factors in eukaryotes can act in oligomeric clusters mediated by molecular crowding and intrinsically disordered protein. This finding impacts on the longstanding puzzle of how transcription factors find their gene targets so efficiently in the complex, heterogeneous environment of the cell.

19 **Abstract**

20 High-speed single-molecule fluorescence microscopy in vivo shows that transcription factors
21 in eukaryotes can act in oligomeric clusters mediated by molecular crowding and intrinsically
22 disordered protein. This finding impacts on the longstanding puzzle of how transcription
23 factors find their gene targets so efficiently in the complex, heterogeneous environment of the
24 cell.

26 **Introduction**

27 Cells regulate gene expression through binding of transcription factors (TFs) to promoters to
28 turn gene expression on or off (1, 2). Simulations show that the time it takes for TFs to find
29 their targets through pure 3D diffusion alone is ~six orders of magnitude larger than what is
30 observed experimentally (3). Hypotheses to explain this observation have included TF
31 heterogeneous mobility comprising a combination of free 3D diffusion combined with sliding
32 and hopping on the DNA plus longer jumps between different DNA strands called
33 intersegment transfer (4–6). In eukaryotic cells, TF localization fluctuates, often between
34 cytoplasm and nucleus (7). Although it has been observed that promoters can pool on the
35 genome in clusters (8) it has not previously been seen that TFs themselves act in clusters, but
36 instead are largely assumed to act as single molecules. Simulations which embody diffusion
37 and binding suggest that multivalent TFs could, in principle, facilitate intersegment transfer
38 (9). Previously, single-molecule fluorescence microscopy has been used to study TF
39 localization in living cells across a range of model organisms, including bacteria, yeast and
40 multi-cellular organisms (10–16). Many studies suggest complexities in diffusion and binding
41 (4, 12, 15, 17, 18) which may include intersegmental transfer (4, 17, 18). However, until now,
42 the direct experimental evidence for intersegmental transfer has been limited.

43 Many of the important features of gene expression control in eukaryotes are
44 exemplified in the model unicellular microorganism *Saccharomyces cerevisiae* (budding
45 yeast). In particular, its glucose sensing pathway presents an experimentally tractable system
46 to study gene regulation. Here, control of gene expression is achieved by TFs which include
47 the Zn finger DNA binding protein Mig1 (19) that acts to repress expression from targets
48 including *GAL* genes involved in glucose metabolism (20). Mig1 localizes towards the
49 nucleus if the extracellular glucose concentration is increased (21), correlated to its own
50 dephosphorylation by a protein called Snf1 (22, 23).

51 In recent investigations from my own group (24) the spatiotemporal dynamics and
52 kinetics of gene regulation in live *S. cerevisiae* cells, using its glucose sensing pathway as a
53 model for signal transduction, was explored using physics methods which enable the
54 understanding of the processes of life one molecule at a time (25, 26), employing ‘single-
55 molecule optical proteomics’ tools (27). The combination of these advanced light microscopy
56 with genetics techniques has previously enabled valuable insights into the activities of several
57 other processes for low copy number proteins (28) in both unicellular organisms and single
58 cells from more complex multicellular organisms (29). These single-molecule/cell and super-
59 resolution microscopy tools have in particular been applied to integrated membrane proteins
60 (30, 31), such as interaction networks like oxidative phosphorylation (32–36), cell division
61 processes (37–39) and protein translocation (40), along with bacterial cell motility (41–44).
62 The tools can also probe the aqueous environment of cells as opposed to just on their
63 hydrophobic cell membrane surface, including processes of DNA
64 replication/remodeling/repair (45–47), and systems more directly relevant to biomedicine
65 such as bacterial infection (48–50).

66 In this Points of View article I discuss further the findings from my team from single-
67 molecule fluorescence microscopy to track functional TFs with very high speed to match

68 typical rates of protein diffusion in live cells and thereby enable ‘blur-free’ observations. We
69 were able to quantify the composition and dynamics of Mig1 under normal and perturbed
70 conditions which affected its state of phosphorylation, and also performed experiments on a
71 protein called Msn2 which functions antagonistically, i.e. instead as an enhancer/activator,
72 for many of the same Mig1 target genes (51) through a completely different signaling
73 pathway. The results showed unexpectedly that Mig1 binds to its target genes as an
74 oligomeric cluster which has stoichiometries in the range ~6-9 molecules. We found evidence
75 that Mig1 molecules in a cluster are glued together through interactions of intrinsically
76 disordered peptide sequences innervated by molecular crowding depletion forces in the cell.
77 Our findings may reveal a more general eukaryotic cell strategy for the control of gene
78 expression which uses intrinsic disorder of many TFs to form clusters that then enable large
79 reductions in the time taken to find a given target gene.

80

81 **Results**

82 **Single-molecule optical proteomics indicates the presence of Mig1 oligomeric clusters**

83 We used millisecond Slimfield single-molecule fluorescence imaging (46, 52, 53) on live *S.*
84 *cerevisiae* cells (Fig. 1A) using a green fluorescent protein (GFP) reporter for Mig1
85 integrated into the genome, including mCherry reporter on the RNA polymerase subunit
86 protein Nrd1 to indicate the position of the cell nucleus. Slimfield was optimized for single-
87 molecule detection sensitivity by using an *in vitro* imaging assay (54). We also measured the
88 maturation effect of the fluorescent proteins in these cells (55) and estimate it to be <15%
89 immature fluorescent protein over the timescale of imaging experiments. Note, Slimfield
90 limits the observation area to an equivalent diameter of <10 μm in the lateral plane to achieve
91 rapid imaging sample times of millisecond and, in some instances sub-millisecond levels
92 (56), but is less ideal to eukaryotic imaging of cells with larger nuclei. A host of other
93 single-molecule techniques based on light-sheet imaging have larger fields of view, and also
94 combine low background and low light toxicity. For the interested reader, these include:
95 HILO (by Tokunaga M.N. et al. (57)), AFM cantilever lightsheet (by Gebhardt, J.C. et al.
96 (11)), lattice light-sheet (by Chen B.C. et al. (58)), multi-focus (by Abrahamsson S. et
97 al.(59)), remote focusing (by Yang et al.(60)), and diagonally scanned light sheet (by Dean et
98 al.(61)).

99 Under depleted /elevated extracellular *glucose* (-/+) we measured cytoplasmic and
100 nuclear Mig1 localization bias respectively, visible in individual cells by our generating rapid
101 microfluidic exchange (a few seconds) of extracellular fluid (Fig. 1B), and resolved two
102 components under both conditions consistent with a diffuse monomeric pool and distinct
103 oligomeric foci of Mig1 (Fig. 1C). The foci were also visible as hotspots using the green-red
104 photoswitchable fluorescent protein mEos2 (62) excited by super-resolution stochastic optical
105 reconstruction microscopy (STORM) (Fig. 1C), with modeling using 3C structural data of the
106 yeast chromosome (63) and sequence alignment analysis for the location of Mig1 target
107 promoters supporting the hypothesis that the majority of Mig1 clusters were specifically
108 binding to Mig1 target genes.

109 Nanoscale tracking determined the position of tracked Mig1 foci to a lateral precision
110 of 40 nm (33, 64) coupled to stoichiometry analysis using stepwise photobleaching of GFP
111 (54) and single cell copy number analysis (65). An additional output from the tracking was
112 the effective diffusion coefficient D as a function of its location in either the cytoplasm,
113 nucleus or translocating across the nuclear envelope, as well as the copy number of Mig1
114 molecules associated with each subcellular region and in each cell as a whole, indicating
115 ~850-1,300 Mig1 molecules per cell dependent on extracellular glucose. It should be noted

116 that confinement may affect the apparent diffusion coefficient in the small volume of a yeast
117 nucleus if the length the mean square displacement (MSD) of tracked particles is comparable
118 to the diameter of the nucleus, however, if our case only the short length scale MSD regions
119 are considered to determine D .

120 In control experiments, a modified strain (51) generated with a binding site for protein
121 PP7 on mRNA produced by one of the Mig1 target genes called *GSY1* showed colocalization
122 between PP7-GFP expressed off a plasmid and Mig1-mCherry expressed genomically under
123 high glucose conditions. We also observed similar clustering and co-localization to PP7 for
124 the antagonistic TF Msn2. These PP7 co-localization results suggest that clusters both of
125 Mig1 and Msn2 are *functionally* active in regulating target gene expression of the test target
126 gene *GSY1*.

127

128 **Cytoplasmic Mig1 diffuses rapidly but nuclear Mig1 can be mobile and immobile**

129 Cytoplasmic Mig1 fluorescent foci at *glucose* (+/-), and nuclear foci at *glucose* (-), were
130 consistent with just a single mobile population whose D of 1-2 $\mu\text{m}^2/\text{s}$ consistent with earlier
131 observations. However, nuclear foci at *glucose* (+) indicated a mixture of mobile and
132 immobile components (Fig. 1D). These results suggested 20-30% of nuclear foci are
133 immobile, consistent with a DNA-bound state. MSD analysis of foci tracks indicated
134 Brownian diffusion over a few tens of ms but increasingly anomalous diffusion over longer
135 timescales, consistent with *glucose* (+) Mig1 diffusion being impacted by interactions with
136 nuclear structures, similar to that reported for other TFs (66). Here, this interaction depended
137 on extracellular glucose despite Mig1 requiring a pathway of proteins to detect it, unlike the
138 more direct detection mechanism of the prokaryotic *lac* repressor. Control experiments with
139 Zn finger deletion strains of Mig1 indicated that Mig1 clusters bind to the DNA via their Zn
140 finger motif with direct glucose dependence. At the high laser excitation intensities used for
141 Slimfield imaging photobleaching is rapid, and so typically a single GFP molecule will
142 photobleach on average after 5-10 consecutive image frame. To account for this we
143 interpolate observed foci brightness values back to the start of each photobleach using an
144 exponential photobleach function. We observed no direct evidence for irreversible
145 photobleaching (i.e. 'photoblinking') with GFP at these intensities, though other fluorescent
146 proteins such as YFP have been known to exhibit such blinking behavior, which if so would
147 need to be further characterized, for example using surface immobilized purified YFP *in*
148 *vitro* samples. A general compromise here, however, is to confine tracking analysis to
149 typically less than 100 ms of laser exposure so that irreversible photoblinking is more
150 dominant than reversible blinking.

151

152

153 **Mig1 nuclear pore complex selectivity is mediated by interactions distant from the** 154 **nuclear envelope**

155 We compared the spatiotemporal dynamics of different Mig1 clusters during translocation by
156 converting trans-nuclear tracks into coordinates parallel and perpendicular to the measured
157 nuclear envelope location, and synchronizing coordinate origins to be at the nuclear envelope
158 crossing point for a given foci track. A heat map of spatial locations of translocating clusters
159 indicated a hotspot of comparable volume to the nuclear pore complexes and accessory
160 structures (67, 68) (Fig. 1E). The dwell time during nuclear envelope translocation was
161 ~ 10 ms, similar to previous estimates for transport factors (69) but here found to be
162 insensitive to glucose (Fig. 1F), demonstrating that there is no direct selectivity on the basis

163 of TF phosphorylation state by nuclear pore complexes themselves which suggests that cargo
164 selectivity mechanisms of nuclear transport (70) are blind to phosphorylation state. Coupled
165 with the observation that Mig1 at *glucose* (-) does not exhibit immobility in the nucleus and
166 that Mig1 lacking the Zn finger still accumulates in the nucleus at *glucose* (+) this suggests
167 that Mig1 localization is driven by changes in Mig1 binding affinity to other proteins, e.g.
168 the general co-repressor complex at the genome (71), or outside the nucleus not involving the
169 nuclear pore complex.

170

171 **Mig1 nuclear clusters turn over in >100 s**

172 By modifying the microscope we were able to implement fluorescence recovery after
173 photobleaching (FRAP) to probe nuclear turnover of Mig1, by focusing a separate laser onto
174 just the nucleus, photobleaching this region with a rapid 200 ms pulse, and quantifying any
175 subsequent fluorescence intensity recovery into that region (Fig. 1G). We could then acquire
176 images with millisecond precision for individual frames but stroboscopically illuminating to
177 extend the range of time scales for recovery before significant GFP photobleaching occurred,
178 enabling FRAP observations at a single-molecule precision to timescales >1,000 s. Analyses
179 demonstrated measurable recovery for both foci and the diffuse pool components in the
180 nucleus, which could be fitted by single exponential functions indicating fast recovery of pool
181 at both *glucose* (-) and (+) with a time constant of just a few seconds but a larger time
182 constant at *glucose* (+) for nuclear foci of at least ~100s (Fig. 1H), with recovery of intensity
183 being consistent with units of ~7-9 GFP molecules for the foci component but no obvious
184 periodicity in stoichiometry measurable from pool recovery. These data suggested that
185 molecular turnover at nuclear foci of Mig1 bound to target genes occurred in units of whole
186 Mig1 clusters.

187

188 **Clusters are stabilized by molecular crowding and intrinsic disorder**

189 Native, denaturing gel electrophoresis and western blots on purified extracts from Mig1-GFP
190 cells (Fig. 1I) indicated a single band corresponding to Mig1. *In vitro* Slimfield imaging of
191 purified Mig1-GFP under identical imaging conditions for live cells similarly indicated
192 monomeric Mig1-GFP foci in addition to a small fraction of brighter foci which were
193 consistent with chance overlap of monomer GFP images. However, addition of a molecular
194 crowding reagent in the form of low molecular weight polyethylene glycol (PEG) at a
195 concentration known to correspond to small molecule 'depletion' forces in cells (72) resulted
196 in significant numbers of oligomers (Fig. 1J), suggesting that Mig1 clusters present in live
197 cells regardless of glucose may be stabilized by depletion components that are lost during
198 biochemical purification.

199 Secondary structure predictions suggested significant regions of disorder away from
200 the Zn finger binding motif. We measured changes in circular dichroism of the Mig1 fusion
201 construct upon addition of PEG (Fig. 1K) in a wavelength range known to be sensitive to
202 transitions between ordered and intrinsically disordered states (73, 74). We also noted similar
203 levels of disorder content in the Msn2 protein far from the Zn finger motif. These
204 observations suggested a TF 'molecular bipolarity', in regards to disorder content, which
205 stabilizes a cluster compact core focused around the disordered regions that undergo a
206 putative phase transition to a more structure state, while exposing Zn fingers and positive
207 surface charges to enable specific and non-specific interactions with accessible DNA strands
208 (Fig. 1L).

210 **Perspective**

211 Our findings address aspects of functional gene regulation in live cells which have hitherto
212 been unexplored, using biophysical technology that has not been available until recently. The
213 results strongly support a functional link between Mig1 and Msn2 TF clusters and target gene
214 expression; a biological role of multivalent TFs for enhancing intersegmental transfer had
215 been elucidated previously in simulations (9) but unobserved experimentally until our
216 discoveries here, and so our findings impact on the longstanding question of how TFs might
217 find their targets in the genome so efficiently. Clustering of a range of nuclear factors has
218 been observed previously using single-molecule techniques, such as transient RNA
219 Polymerase II cluster dynamics in living cells using time-correlated PALM (tc-PALM) (75,
220 76). Also functional nuclear protein clusters have been seen (77) and the Bicoid transcription
221 factor in fruit fly embryos has been observed to form clusters mediated in part mediated by
222 intrinsically disordered peptide sequences (78).

223 Quantifying nearest-neighbor distances between Mig1 promoter sites in the *S.*
224 *cerevisiae* genome from the 3C model indicates 20-30% are <50 nm apart, small enough to
225 enable different DNA segments to be linked though intersegment transfer by a single cluster
226 (6, 9), which would also enable in principle simultaneous binding of >1 gene target from just
227 a single TF cluster. There is a net positive charge in the vicinity of Zn finger motifs, and this
228 would also enable non-specific electrostatic interactions with the negatively charged
229 phosphate backbone of DNA, facilitating 1D sliding diffusion of the protein along a DNA
230 strand. Thus, a cluster may be able to slide along DNA in a largely sequence-independent
231 manner and undergo intersegmental transfer to a neighboring strand relatively easily, either
232 spontaneously or stimulated by the presence of protein barriers on the DNA in a process
233 likely to have some sequence dependence when an obstacle is encountered. In particular,
234 bound RNA polymerases present during gene transcription at sequence specific sites could
235 act as roadblocks to kick off translocating clusters from a DNA strand, to again facilitate
236 intersegmental transfer and thus increase the ultimate chances that TF clusters will encounter
237 one of the gene targets and specifically bind via the Zn finger motif, thus predominantly
238 circumventing the requirement for significant amounts of slow 3D diffusion in the
239 nucleoplasm.

240 Our discovery is, to our knowledge, the first to make a link between predicted disorder
241 and the ability to form oligomeric clusters in TFs. Our findings may potentially offer some
242 insights into addressing the longstanding question of why in general there is so much
243 predicted disorder in eukaryote transcription factors; ~90% of eukaryotic TFs indicate
244 significant proportions of sequences with disordered content (79). Our finding that protein
245 interactions based on relatively weak molecular crowding depletion forces has functional
246 relevance in several areas of cell biology, such as processes involving aggregation mediated
247 through intrinsic disorder interactions; for example, those of amyloid plaques found in
248 neurodegenerative disorders including Alzheimer's and Parkinson's diseases (80). Increased
249 understanding of the clustering mechanism might therefore be of value in understanding the
250 progression of these diseases. Open questions remain though: for example, are clusters homo-
251 oligomeric or do they contain multiple different TFs? How is specificity maintained inside a
252 cluster? Are the components of the clusters themselves dynamic and undergo molecular
253 turnover? Can the ability to cluster be controlled, for example by switching the state of
254 phosphorylation?
255

256 **Acknowledgments**

257 The work of the original research article described (24) also involved Adam Wollman,
258 Sviatlana Shashkova, Erik Hedlund, Rosemarie Friemann and Stefan Hohmann, and the
259 Bioscience Technology Facility of the University of York, UK. Thanks to Mark Johnston
260 (CU Denver) for a Mig1 phosphorylation mutant plasmid, and Michael Elowitz (Caltech) for
261 a Mig1/Msn2/PP7 and Zn finger deletion strain.

262

263 **Funding**

264 Supported by the Biological Physical Sciences Institute, Royal Society, MRC (grant
265 MR/K01580X/1), BBSRC (grant BB/N006453/1), Swedish Research Council and European
266 Commission via Marie Curie-Network for Initial training ISOLATE (Grant agreement nr:
267 289995) and the Marie Curie Alumni Association.

268

269 **Conflict of interest**

270 There are no conflicts of interests.

271

272 **References**

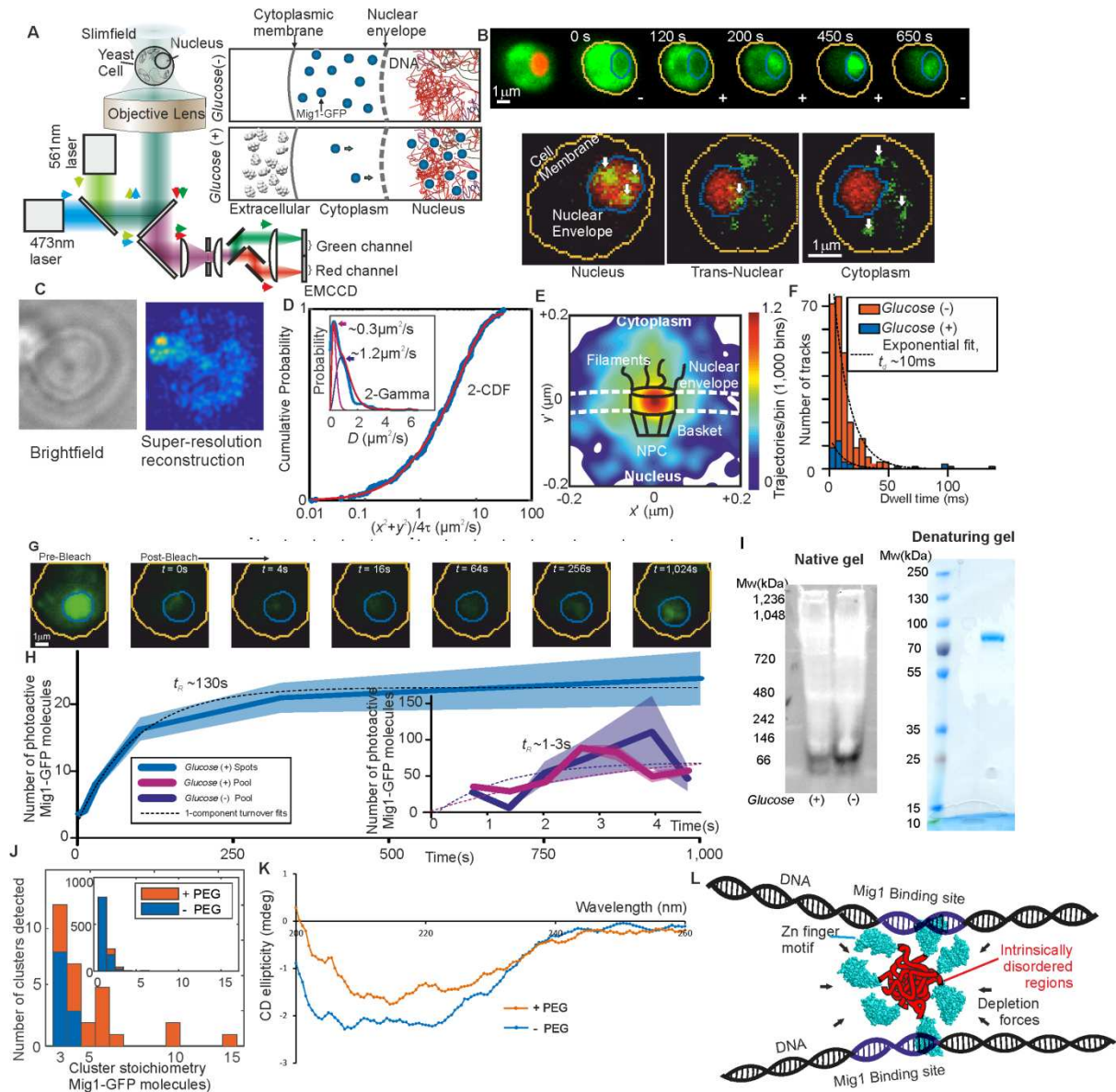
- 273 1. F. Jacob, J. Monod, Genetic regulatory mechanisms in the synthesis of proteins. *J.*
274 *Mol. Biol.* **3**, 318–356 (1961).
- 275 2. J. Gertz, E. D. Siggia, B. A. Cohen, Analysis of combinatorial cis-regulation in
276 synthetic and genomic promoters. *Nature*. **457**, 215–8 (2009).
- 277 3. O. G. Berg, R. B. Winter, P. H. Von Hippel, Diffusion-driven mechanisms of protein
278 translocation on nucleic acids. 1. Models and theory. *Biochemistry*. **20**, 6929–6948
279 (1981).
- 280 4. A. Mahmutovic, O. G. Berg, J. Elf, What matters for lac repressor search in vivo--
281 sliding, hopping, intersegment transfer, crowding on DNA or recognition? *Nucleic*
282 *Acids Res.* **43**, 3454–64 (2015).
- 283 5. S. E. Halford, J. F. Marko, How do site-specific DNA-binding proteins find their
284 targets? *Nucleic Acids Res.* **32**, 3040–52 (2004).
- 285 6. D. M. Gowers, S. E. Halford, Protein motion from non-specific to specific DNA by
286 three-dimensional routes aided by supercoiling. *EMBO J.* **22**, 1410–8 (2003).
- 287 7. S. T. Whiteside, S. Goodbourn, Signal transduction and nuclear targeting: regulation of
288 transcription factor activity by subcellular localisation. *J. Cell Sci.* **104** (Pt 4, 949–55
289 (1993).
- 290 8. C. T. Harbison *et al.*, Transcriptional regulatory code of a eukaryotic genome. *Nature*.
291 **431**, 99–104 (2004).
- 292 9. H. G. Schmidt, S. Sewitz, S. S. Andrews, K. Lipkow, An Integrated Model of
293 Transcription Factor Diffusion Shows the Importance of Intersegmental Transfer and
294 Quaternary Protein Structure for Target Site Finding. **9**, e108575 (2014).
- 295 10. G.-W. Li, X. S. Xie, Central dogma at the single-molecule level in living cells. *Nature*.
296 **475**, 308–15 (2011).
- 297 11. J. C. M. Gebhardt *et al.*, Single-molecule imaging of transcription factor binding to
298 DNA in live mammalian cells. *Nat. Methods*. **10**, 421–426 (2013).

- 299 12. D. Normanno *et al.*, Probing the target search of DNA-binding proteins in mammalian
300 cells using TetR as model searcher. *Nat. Commun.* **6**, 7357 (2015).
- 301 13. D. Mazza, A. Abernathy, N. Golob, T. Morisaki, J. G. McNally, A benchmark for
302 chromatin binding measurements in live cells. *Nucleic Acids Res.* **40**, e119 (2012).
- 303 14. Z. Liu *et al.*, 3D imaging of Sox2 enhancer clusters in embryonic stem cells. *Elife.* **3**,
304 e04236 (2014).
- 305 15. J. Chen *et al.*, Single-Molecule Dynamics of Enhanceosome Assembly in Embryonic
306 Stem Cells. *Cell.* **156**, 1274–1285 (2014).
- 307 16. Z. Zhang *et al.*, Rapid dynamics of general transcription factor TFIIB binding during
308 preinitiation complex assembly revealed by single-molecule analysis. *Genes Dev.* **30**,
309 2106–2118 (2016).
- 310 17. P. Hammar *et al.*, The lac repressor displays facilitated diffusion in living cells.
311 *Science.* **336**, 1595–8 (2012).
- 312 18. J. C. M. Gebhardt *et al.*, Single-molecule imaging of transcription factor binding to
313 DNA in live mammalian cells. *Nat. Methods.* **10**, 421–6 (2013).
- 314 19. J. O. Nehlin, M. Carlberg, H. Ronne, Control of yeast GAL genes by MIG1 repressor:
315 a transcriptional cascade in the glucose response. *EMBO J.* **10**, 3373–7 (1991).
- 316 20. E. Frolova, Binding of the glucose-dependent Mig1p repressor to the GAL1 and GAL4
317 promoters in vivo: regulation by glucose and chromatin structure. *Nucleic Acids Res.*
318 **27**, 1350–1358 (1999).
- 319 21. M. J. De Vit, J. a Waddle, M. Johnston, Regulated nuclear translocation of the Mig1
320 glucose repressor. *Mol. Biol. Cell.* **8**, 1603–18 (1997).
- 321 22. L. Bendrioua *et al.*, Yeast AMP-activated Protein Kinase Monitors Glucose
322 Concentration Changes and Absolute Glucose Levels. *J. Biol. Chem.* **289**, 12863–75
323 (2014).
- 324 23. S. Shashkova, A. J. M. Wollman, M. C. Leake, S. Hohmann, The yeast Mig1
325 transcriptional repressor is dephosphorylated by glucose-dependent and -independent
326 mechanisms. *FEMS Microbiol. Lett.* **364** (2017), doi:10.1093/femsle/fnx133.
- 327 24. A. J. M. J. Wollman *et al.*, Transcription factor clusters regulate genes in eukaryotic
328 cells. **6**, e27451 (2017).
- 329 25. M. C. Leake, The physics of life: one molecule at a time. *Philos. Trans. R. Soc. Lond.*
330 *B. Biol. Sci.* **368**, 20120248 (2013).
- 331 26. H. Miller, Z. Zhou, J. Shepherd, A. J. M. Wollman, M. C. Leake, Single-molecule
332 techniques in biophysics: a review of the progress in methods and applications.
333 *Reports Prog. Phys.* **81**, 24601 (2018).
- 334 27. S. Shashkova, M. C. Leake, Single-molecule fluorescence microscopy review:
335 Shedding new light on old problems. *Biosci. Rep.* **37** (2017),
336 doi:10.1042/BSR20170031.
- 337 28. B. Huang *et al.*, Counting Low-Copy Number Proteins in a Single Cell. *Science.* **315**,
338 81–4 (2007).
- 339 29. M. Wu, A. K. Singh, Single-cell protein analysis. *Curr. Opin. Biotechnol.* **23**, 83–8
340 (2012).

- 341 30. S. J. Bryan *et al.*, Localisation and interactions of the Vipp1 protein in cyanobacteria.
342 *Mol. Microbiol.* **94**, 1179–1195 (2014).
- 343 31. A. Nenner *et al.*, Independent mobility of proteins and lipids in the plasma
344 membrane of *Escherichia coli*. *Mol. Microbiol.* **92**, 1142–53 (2014).
- 345 32. T. Lenn, M. C. Leake, Single-molecule studies of the dynamics and interactions of
346 bacterial OXPHOS complexes. *Biochim. Biophys. Acta - Bioenerg.* **1857**, 224–231
347 (2016).
- 348 33. I. Llorente-Garcia *et al.*, Single-molecule in vivo imaging of bacterial respiratory
349 complexes indicates delocalized oxidative phosphorylation. *Biochim. Biophys. Acta.*
350 **1837**, 811–24 (2014).
- 351 34. Y. T. Lenn, M. C. Leake, C. W. Mullineaux, Are *Escherichia coli* OXPHOS
352 complexes concentrated in specialized zones within the plasma membrane? *Biochem.*
353 *Soc. Trans.* **36**, 1032–6 (2008).
- 354 35. T. Lenn, M. C. Leake, C. W. Mullineaux, Clustering and dynamics of cytochrome bd-I
355 complexes in the *Escherichia coli* plasma membrane in vivo. *Mol. Microbiol.* **70**,
356 1397–407 (2008).
- 357 36. A. Badrinarayanan, M. C. Leake, Using Fluorescence Recovery After Photobleaching
358 (FRAP) to Study Dynamics of the Structural Maintenance of Chromosome (SMC)
359 Complex In Vivo. *Methods Mol. Biol.* **1431**, 37–46 (2016).
- 360 37. S.-W. S.-W. Chiu, M. A. J. Roberts, M. C. Leake, J. P. Armitage, Positioning of
361 chemosensory proteins and ftsz through the *Rhodobacter sphaeroides* cell cycle. *Mol.*
362 *Microbiol.* **90**, 322–37 (2013).
- 363 38. A. W. Bisson-Filho *et al.*, Treadmilling by FtsZ filaments drives peptidoglycan
364 synthesis and bacterial cell division. *Science.* **355**, 739–743 (2017).
- 365 39. V. A. Lund *et al.*, Molecular coordination of *Staphylococcus aureus* cell division.
366 *Elife.* **7**, e32057 (2018).
- 367 40. M. C. Leake *et al.*, Variable stoichiometry of the TatA component of the twin-arginine
368 protein transport system observed by in vivo single-molecule imaging. *Proc. Natl.*
369 *Acad. Sci. U. S. A.* **105**, 15376–81 (2008).
- 370 41. S. W. W. Reid *et al.*, The maximum number of torque-generating units in the flagellar
371 motor of *Escherichia coli* is at least 11. *Proc. Natl. Acad. Sci. U. S. A.* **103**, 8066–71
372 (2006).
- 373 42. Y. Sowa *et al.*, Direct observation of steps in rotation of the bacterial flagellar motor.
374 *Nature.* **437**, 916–9 (2005).
- 375 43. T. Pilizota *et al.*, A molecular brake, not a clutch, stops the *Rhodobacter sphaeroides*
376 flagellar motor. *Proc. Natl. Acad. Sci. U. S. A.* **106**, 11582–7 (2009).
- 377 44. C.-J. Lo, M. C. Leake, T. Pilizota, R. M. Berry, Nonequivalence of membrane voltage
378 and ion-gradient as driving forces for the bacterial flagellar motor at low load.
379 *Biophys. J.* **93**, 294–302 (2007).
- 380 45. R. Reyes-Lamothe, D. J. Sherratt, M. C. Leake, Stoichiometry and architecture of
381 active DNA replication machinery in *Escherichia coli*. *Science.* **328**, 498–501 (2010).
- 382 46. A. Badrinarayanan, R. Reyes-Lamothe, S. Uphoff, M. C. Leake, D. J. Sherratt, In vivo
383 architecture and action of bacterial structural maintenance of chromosome proteins.

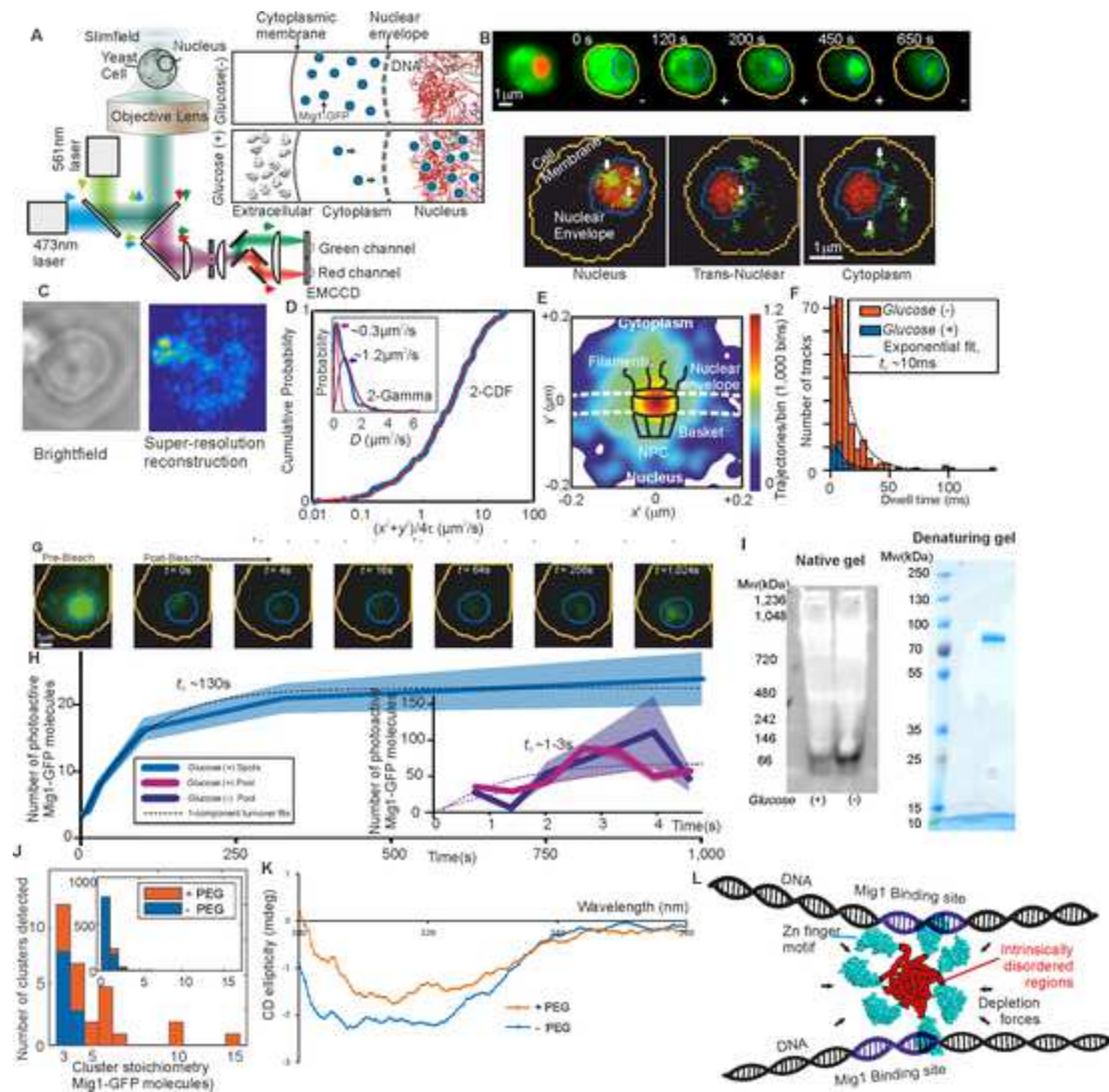
- 384 *Science*. **338**, 528–31 (2012).
- 385 47. A. J. M. Wollman, A. H. Syeda, P. McGlynn, M. C. Leake, Single-molecule
386 observation of DNA replication repair pathways in *E. coli*. *Adv. Exp. Med. Biol.* **915**,
387 5–16 (2016).
- 388 48. M. C. Leake, The Biophysics of Infection. *Adv. Exp. Med. Biol.* **915**, 1–3 (2016).
- 389 49. H. Miller, A. J. M. Wollman, M. C. Leake, Designing a Single-Molecule Biophysics
390 Tool for Characterising DNA Damage for Techniques that Kill Infectious Pathogens
391 Through DNA Damage Effects. *Adv. Exp. Med. Biol.* **915**, 115–27 (2016).
- 392 50. A. J. M. Wollman, H. Miller, S. Foster, M. C. Leake, An automated image analysis
393 framework for segmentation and division plane detection of single live *Staphylococcus*
394 *aureus* cells which can operate at millisecond sampling time scales using bespoke
395 Slimfield microscopy. *Phys. Biol.* **5**, 55002 (2016).
- 396 51. Y. Lin, C. H. Sohn, C. K. Dalal, L. Cai, M. B. Elowitz, Combinatorial gene regulation
397 by modulation of relative pulse timing. *Nature*. **527**, 54–58 (2015).
- 398 52. M. Plank, G. H. Wadhams, M. C. Leake, Millisecond timescale slimfield imaging and
399 automated quantification of single fluorescent protein molecules for use in probing
400 complex biological processes. *Integr. Biol. (Camb)*. **1**, 602–12 (2009).
- 401 53. R. Reyes-Lamothe, D. J. Sherratt, M. C. Leake, Stoichiometry and architecture of
402 active DNA replication machinery in *Escherichia coli*. *Science*. **328**, 498–501 (2010).
- 403 54. M. C. Leake *et al.*, Stoichiometry and turnover in single, functioning membrane
404 protein complexes. *Nature*. **443**, 355–358 (2006).
- 405 55. S. Shashkova, A. Wollman, S. Hohmann, M. C. Leake, Characterising Maturation of
406 GFP and mCherry of Genomically Integrated Fusions in *Saccharomyces cerevisiae*.
407 *Bio Protoc.* **7**, e27110 (2018).
- 408 56. H. Miller, J. Cosgrove, A. Wollman, E. Taylor, P. O’Toole, M. Coles, M. C. Leake.
409 High-speed single-molecule tracking of CXCL13 in the B-Follicle. *Front. Immunol.*,
410 in press (2018).
- 411 57. M. Tokunaga, N. Imamoto, K. Sakata-Sogawa, Highly inclined thin illumination
412 enables clear single-molecule imaging in cells. *Nat. Methods*. **5**, 159–161 (2008).
- 413 58. B.-C. Chen *et al.*, Lattice light-sheet microscopy: imaging molecules to embryos at
414 high spatiotemporal resolution. *Science*. **346**, 1257998 (2014).
- 415 59. S. Abrahamsson *et al.*, Fast multicolor 3D imaging using aberration-corrected
416 multifocus microscopy. *Nat. Methods*. **10**, 60–63 (2013).
- 417 60. B. Yang *et al.*, High Numerical Aperture Epi-illumination Selective Plane Illumination
418 Microscopy. *bioRxiv*, 273359 (2018).
- 419 61. K. M. Dean *et al.*, Diagonally Scanned Light-Sheet Microscopy for Fast Volumetric
420 Imaging of Adherent Cells. *Biophys. J.* **110**, 1456–1465 (2016).
- 421 62. S. A. McKinney, C. S. Murphy, K. L. Hazelwood, M. W. Davidson, L. L. Looger, A
422 bright and photostable photoconvertible fluorescent protein. *Nat. Methods*. **6**, 131–3
423 (2009).
- 424 63. Z. Duan *et al.*, A three-dimensional model of the yeast genome. *Nature*. **465**, 363–7
425 (2010).

- 426 64. H. Miller, Z. Zhou, A. J. M. Wollman, M. C. Leake, Superresolution imaging of single
427 DNA molecules using stochastic photoblinking of minor groove and intercalating
428 dyes. *Methods*. **88**, 81–8 (2015).
- 429 65. A. J. M. Wollman, M. C. Leake, Millisecond single-molecule localization microscopy
430 combined with convolution analysis and automated image segmentation to determine
431 protein concentrations in complexly structured, functional cells, one cell at a time.
432 *Faraday Discuss.* **184**, 401–24 (2015).
- 433 66. I. Izeddin *et al.*, Single-molecule tracking in live cells reveals distinct target-search
434 strategies of transcription factors in the nucleus. *Elife*. **3**, e02230 (2014).
- 435 67. S. A. Adam, The nuclear pore complex. *Genome Biol.* **2**, reviews0007.1-
436 reviews0007.7 (2001).
- 437 68. C. Strambio-De-Castillia, M. Niepel, M. P. Rout, The nuclear pore complex: bridging
438 nuclear transport and gene regulation. *Nat. Rev. Mol. Cell Biol.* **11**, 490–501 (2010).
- 439 69. W. Yang, J. Gelles, S. M. Musser, Imaging of single-molecule translocation through
440 nuclear pore complexes. *Proc. Natl. Acad. Sci. U. S. A.* **101**, 12887–12892 (2004).
- 441 70. A. R. Lowe *et al.*, Selectivity mechanism of the nuclear pore complex characterized by
442 single cargo tracking. *Nature*. **467**, 600–603 (2010).
- 443 71. M. A. Treitel, M. Carlson, Repression by SSN6-TUP1 is directed by MIG1, a
444 repressor/activator protein. *Proc. Natl. Acad. Sci. U. S. A.* **92**, 3132–6 (1995).
- 445 72. Y. Phillip, G. Schreiber, Formation of protein complexes in crowded environments--
446 from in vitro to in vivo. *FEBS Lett.* **587**, 1046–52 (2013).
- 447 73. K. Sode, S. Ochiai, N. Kobayashi, E. Usuzaka, Effect of reparation of repeat sequences
448 in the human alpha-synuclein on fibrillation ability. *Int. J. Biol. Sci.* **3**, 1–7 (2007).
- 449 74. C. Avitabile *et al.*, Circular Dichroism studies on the interactions of antimicrobial
450 peptides with bacterial cells. *Sci. Rep.* **4**, 337–360 (2014).
- 451 75. I. I. Cisse *et al.*, Real-Time Dynamics of RNA Polymerase II Clustering in Live
452 Human Cells. *Science*. **341**, 664–667 (2013).
- 453 76. W.-K. Cho *et al.*, RNA Polymerase II cluster dynamics predict mRNA output in living
454 cells. *Elife*. **5**, e13617 (2016).
- 455 77. J. Qian *et al.*, B Cell Super-Enhancers and Regulatory Clusters Recruit AID
456 Tumorigenic Activity. *Cell*. **159**, 1524–1537 (2014).
- 457 78. M. Mir *et al.*, Dense Bicoid Hubs Accentuate Binding along the Morphogen Gradient.
458 *Genes & Dev.* **31**, 1784–94 (2017).
- 459 79. J. Liu *et al.*, Intrinsic disorder in transcription factors. *Biochemistry*. **45**, 6873–88
460 (2006).
- 461 80. V. N. Uversky, V. B. Patel, Intrinsically disordered proteins and their (disordered)
462 proteomes in neurodegenerative disorders. *Front Aging Neurosci.* **7**, 18 (2015).
- 463 81. M. C. Leake, D. Wilson, M. Gautel, R. M. Simmons, The elasticity of single titin
464 molecules using a two-bead optical tweezers assay. *Biophys. J.* **87**, 1112–35 (2004).
- 465 82. M. C. Leake, D. Wilson, B. Bullard, R. M. Simmons, The elasticity of single kettin
466 molecules using a two-bead laser-tweezers assay. *FEBS Lett.* **535**, 55–60 (2003).
- 467



468

469 **Figure 1.** TFs form clusters in eukaryotic cell. (A) Schematic of millisecond Slimfield
 470 microscopy. (B) Fluorescence imaging of Mig1-GFP (green) with nucleus indicated (red) by
 471 Nrd1-mCherry, showing different cellular locations, stoichiometry determined by step-wise
 472 photobleaching that can be measured using Fourier analysis and edge-detection filters (54,
 473 81, 82). (C) STORM imaging using Mig1-mEos2. (D) Mobility analysis for cumulative
 474 distribution function (CDF) and Gamma fits. (E) Mig-GFP localization through a nuclear
 475 pore complex. (F) Dwell time for tracks translocating the nuclear envelope. (G) Images and
 476 (H) analysis for FRAP indicating turnover of nuclear Mig1-GFP. (I) Native and denaturing
 477 gels on purified Mig1-GFP. (J) Mig1-GFP cluster stoichiometry in presence/absence of
 478 molecular crowding. (K) Circular dichroism spectra in presence/absence of molecular
 479 crowding. (L) Cartoon model for shape of a Mig1 cluster in vicinity of DNA strands.





1
2
3
4
5
6
7
8
9
10
11
12
13
14
15
16
17
18
19
20
21
22
23
24
25
26
27
28
29
30
31
32
33
34
35
36
37
38
39
40
41
42
43
44
45
46
47
48
49
50
51
52
53
54
55
56
57
58
59
60
61
62
63
64
65

From: *Professor Mark C. Leake FInstP, FRMS, FRSB, PhD*
Tel: +44 (0) 1904 322697/328566
Fax: +44 (0) 1904 322214
Email: mark.leake@york.ac.uk
Institute: <http://www.york.ac.uk/physics/bpsi>
Group: <http://single-molecule-biophysics.org>

Director, Biological Physical Sciences Institute (BPSI)
Chair of Biological Physics
Departments of Physics and Biology
University of York
Heslington
York YO10 5DD, UK

Monday, 30 April 2018

In reference to: Reviewer comments for “**Transcription factors in eukaryotic cells can functionally regulate gene expression by acting in oligomeric assemblies formed from an intrinsically disordered protein phase transition enabled by molecular crowding**”

Alberto Kornblihtt

Dear Alberto

Many thanks for supplying the reviewer feedback: they were very helpful. I have revised the piece accordingly, and it is improved as a result. Please find overleaf a point by point response to all the reviewer comments.

If I may be of any further assistance please do not hesitate to contact me.

Yours sincerely,

Prof. Mark C. Leake

.***

Reviewer 1:

1 Here is a small list of omitted citations on this subject that should be included to make the review more
2 fairly
3 balanced:

4 GR (Gebhardt, J.C. et al. <https://www.nature.com/articles/nmeth.2411>)
5 TetR (Normanno, D. et al. <https://www.nature.com/articles/ncomms8357>)
6 p53 (Mazza, D. et al. <https://www.ncbi.nlm.nih.gov/pmc/articles/PMC3424588/>)
7 Sox2 (Liu Z. et al. <https://elifesciences.org/articles/04236>
8 and
9 Chen J. et al. <https://www.ncbi.nlm.nih.gov/pubmed/24630727>)
10 TFIIIB
11 (by Zhang Z. et al. <http://genesdev.cshlp.org/content/30/18/2106>)
12
13

14 These references have now been added

15
16 2. The only imaging modality presented in this mini-review is Slimfield. This technique limits the
17 observation area to a
18 few micrometers, and hence is unsuitable to eukaryotic imaging of cells with larger nuclei. A host of
19 other single-molecule
20 techniques based on light-sheet imaging have much bigger fields of view, and have the added
21 advantage of
22 low background and low light toxicity.
23 Here are omitted references of imaging modalities that have been recently implemented to image
24 eukaryotic nuclei:

25 HILO
26 (by Tokunaga M.N. et al. <https://www.nature.com/articles/nmeth1171>)
27 AFM cantilever light-sheet
28 (by Gebhardt, J.C. et al. <https://www.nature.com/articles/nmeth.2411>)
29 lattice light-sheet
30 (by Chen B.C. et al. <http://science.sciencemag.org/content/346/6208/1257998>)
31 multi-focus
32 (by Abrahamsson S. et al. <https://www.nature.com/articles/nmeth.2277>)
33 remote focusing
34 (by Yang et al. <https://www.biorxiv.org/content/early/2018/02/28/273359>)
35 diagonally scanned light sheet
36 (by Dean et al. <https://doi.org/10.1016/j.bpj.2016.01.029>)
37
38

39 These references have now been added

40
41
42 3. Paragraph lines 50-64. Confusing mix of references for different model organisms: yeast, multi-
43 cellular, and bacterial)

44
45 I have now clarified that these references refer to a range of different model organisms

46
47 4. Paragraph lines 114-126. The review should highlight how confinement affects apparent diffusion
48 coefficient in the small volume of a yeast nucleus.

49 This has now been added

50
51 5. Paragraph lines 128-144. The review should state how bleaching and dye-photophysics (blinking,
52 dark-state transitions) are accounted for. This is especially relevant for Slimfield imaging conditions of
53 high laser power densities.

54 Discussion has been added here concerning how blinking and bleaching dye photophysics are
55 accounted for.
56

57
58 6. Line 194: References 63 and 64 do not in fact argue for the static "transcription factories". These
59 papers rather should be cited for time-correlated PALM (tc-PALM), which accurately accounts for dye-
60 photophysics, and describe live cell RNA Polymerase II cluster dynamics that are quite transient.

61 This has now been added
62
63
64
65

7. Lines 33-34: Eukaryotic TFs do not always fluctuate between cytoplasm and the nucleus.

This has now been corrected

8. Line 88: The author should address how <15 % fluorophore maturation is compatible with single-molecule counting.

The '<15%' refers to the immature fluorescent protein level – this has now been clarified

1
2
3
4
5
6
7
8
9
10
11
12
13
14
15
16
17
18
19
20
21
22
23
24
25
26
27
28
29
30
31
32
33
34
35
36
37
38
39
40
41
42
43
44
45
46
47
48
49
50
51
52
53
54
55
56
57
58
59
60
61
62
63
64
65